



HAL
open science

Synthesis, characterization and optical behaviour of vapour grown nano-crystalline Al–Cr–Fe–Mo thin films

Valerie Brien, S. Kenzari, P. Weisbecker, Sébastien J. Weber, F. Machizaud, J.-M. Dubois

► **To cite this version:**

Valerie Brien, S. Kenzari, P. Weisbecker, Sébastien J. Weber, F. Machizaud, et al.. Synthesis, characterization and optical behaviour of vapour grown nano-crystalline Al–Cr–Fe–Mo thin films. *Journal of Alloys and Compounds*, 2005, 391 (1-2), pp.206-211. 10.1016/j.jallcom.2004.08.085 . hal-02882473

HAL Id: hal-02882473

<https://hal.science/hal-02882473>

Submitted on 22 Oct 2020

HAL is a multi-disciplinary open access archive for the deposit and dissemination of scientific research documents, whether they are published or not. The documents may come from teaching and research institutions in France or abroad, or from public or private research centers.

L'archive ouverte pluridisciplinaire **HAL**, est destinée au dépôt et à la diffusion de documents scientifiques de niveau recherche, publiés ou non, émanant des établissements d'enseignement et de recherche français ou étrangers, des laboratoires publics ou privés.

.Synthesis, characterization and optical behaviour of vapour grown nano-crystalline
Al-Cr-Fe-Mo thin films

V. Brien^{a,*}, S. Kenzari^a, P. Weisbecker^a, S. Weber^b, F. Machizaud^a and J.-M. Dubois^a

a Laboratoire de Science et Génie des Matériaux et de Métallurgie, UMR 7584, CNRS-INPL-UHP, Parc de Saurupt, ENSMN, 54042 NANCY Cedex, France

b Laboratoire de Physique des Matériaux, UMR 7556, CNRS-INPL-UHP, Parc de Saurupt, ENSMN, 54042 NANCY Cedex, France

* Corresponding author : E-mail-: Valerie.Brien@lpmi.uhp-nancy.fr

Tel : + 33.3.83.68.49.28

Fax : + 33.3.83.68.49.33

Abstract

Thermal evaporation process was employed in production of thin films of an Al-Cr-Fe-Mo alloy. Microstructural and chemical features were respectively evaluated by grazing X-ray diffraction, transmission electron microscopy and sputtered neutral mass spectroscopy. Solidification structures reveal a homogeneous nanosized (2 - 70 nm) granular morphology. Experimental synthesis parameters leading to films purely made of the known O₁ approximant phase have been defined. The other films were made of two phase particles, ie. O₁ grains mixed with pure cubic aluminium grains. Optical reflectance of the O₁ film over the infra-red and visible wavelength domains is presented.

Keywords: A. thin films, B. vapour deposition; C. Scanning and transmission electron microscopy; C. X-ray diffraction

¹ Now at : LABORATOIRE de PHYSIQUE des MILIEUX IONISES et APPLICATIONS, UMR 7040 CNRS-UHP – Université Henri Poincaré Nancy I, Faculté des Sciences B.P. 239 – 54506 VANDOEUVRE LES NANCY Cedex

1. Introduction

Glass industries are highly interested in modifying surface and optical properties of their glass in order to produce new products for new markets. Such added value can be performed depositing a coating of a well-chosen material. Many studies on quasicrystals and, more and more commonly, their approximant phases show their growing importance in the coating technology owing to their appropriate properties [1-11]. For instance, their low adhesion, high hardness, excellent corrosion resistance and reduced optical conductivity at low frequencies make them very attractive for forming films on substrates [12-16]. Indeed, optical properties of quasicrystalline matter, and approximant phases compared to the one of the metallic constituents, exhibit an important absorption (40 % in infra-red domain) [14,17-20]. This ability could be exploited for making infra-red absorbers. Such an advantage combined with good corrosion behaviour thanks to particular chemical species is attractive. Previous work has already been performed on Al-Cr-Fe films showing it was possible to get as-deposited Al-Cr-Fe approximant thin films grown from the vapour phase on glass substrates [15,16]. The obtained films were made of a mixture of approximant phases and were shown to exhibit the optical properties of approximant phases over the visible domain. They could however not be tested in the infra-red domain as they were not thick enough implying so an alteration of the optical measurements due to the glass substrate. The Al-Cr-Fe, like the Al-Cr-Fe-Cu system is rich in approximant phases of the decagonal phase (O_1 , O_2 , γ brass...) [15,18,21]. The idea here is to be able to get a thick enough film made of a single phase, either approximant or quasicrystalline (decagonal, icosahedral). The challenge is also to explore the possibility to extend the corrosion resistance of this approximant hoping a substitution of Cr by the iso-electronic atom Mo in order to investigate modifications (and improvement) in terms of physical and chemical properties.

2. Experiment

2.1. Techniques of preparation

Thermal evaporation was performed in an Edwards AUTO 306 vacuum coater using tungsten filaments. The evaporation set-up allows the heating of the substrate thanks to Joule effect up to 320°C. Heating is produced by a resistance located just behind the holders. The temperature of the substrate T_s was controlled by the means of a thermocouple located behind and in contact with the substrate holders. The set-up also allows the control of the distance d between the source and the substrate. Vacuum condition before deposition was 10^{-7} mbar. The films were deposited on glass substrates. They were produced from small pieces of matter (50 mg) placed on tungsten basket. These pieces were cut out of an ingot obtained by radio-frequency melting, by mixing high purity elements (99.999 % for Al, 99.99% for Cr and Fe and 99.95% for Mo) under helium atmosphere in an induction copper furnace cooled by interior water circulation. Different nominal compositions were tried aiming at a composition near the known one of the Al-Cr-Fe/O₁-phase: Al_{82.8}Cr_{13.9}Fe_{3.2} [15, 16] to prepare the films: Al_{72.5}Cr₂₀Fe₆Mo_{1.5}, Al₇₀Cr₁₈Fe₇Mo₅, Al₆₈Cr₂₀Fe₇Mo₅, Al₆₆Cr₂₂Fe₇Mo₅ and Al₇₄Cr₁₀Fe₆Mo₁₀. Due to the observed relative abilities of elements to condense on substrates (after chemical SNMS expertise - cf. section 2.2- performed on films) the ingot of nominal composition Al₇₄Cr₁₀Fe₆Mo₁₀ was chosen for the preparation of the evaporated films. Its chemical composition and distribution of the elements were checked by Electron Probe Microanalysis (EPMA) (precision on chemical composition is 1 at.%). X-ray diffraction ($\theta - 2\theta$) and Field Emission Gun Scanning Electron Microscopy (FEG-SEM) analyses show that the ingot is made of two main phases (cf. Figure 1). One of them is an orthorhombic approximant of the decagonal phase. Such a checking lead us to show that sufficient homogenization of the ingots could be achieved by performing three melts. Each melt was followed by a cooling down in the induction furnace (see § 3.1).

2.2. Techniques of characterization

Chemical depth profiles of the films were obtained by Sputtered Neutral Mass Spectroscopy (SNMS). All the chemical compositions are given within an experimental error of 5 at. %. The thickness of the films was estimated by performing profilometry on the SNMS craters and was found to be in the 50-200 nm range. Grazing incidence X-Ray Diffraction (GXR) using the $\text{CoK}_{\alpha 1}$ radiation and a curved detector (INEL CPS120) was performed at 0.5° incidence for the identification of the phases. Carbon coated copper electron microscopy grids were systematically placed just next to the film on the substrate holder to perform transmission electron diffraction and imaging. Transmission Electron Microscopy (TEM) observations were carried out on a PHILIPS CM200 microscope. An accelerating voltage of 200 kV was used. EDS spectra recorded in the analyzed zones do not exhibit a copper signal, which proves that no copper diffusion in the film from the grid occurred. In order to get a complementary overview of films, they were all systematically analysed by these four techniques (cf. Table 1). The reflectance spectra were measured at room temperature using a Perkin-Elmer spectrometer on the 200 – 2600 nm range at nearly normal incidence.

3. Results and discussion

3.1 Control of the chemistry and homogeneity of the source matter

The chemical dispersion studied by EPMA shows that an ingot prepared by radio-frequency melting in the used copper furnace exhibits chemical gradients from the core towards the external part. These gradients follow a radial symmetry lead by the geometry of the cooling device. Fig. 1a shows the transverse shape of such an ingot. It appears three consecutive meltings are necessary to reach a sufficient chemical homogenization. EPMA results of analysis performed along the lines 1, 2 and 3, which have been drawn in fig.1.a, can be seen in Fig. 1(b). 50 mg of matter approximately correspond to a volume like a piece

whose diameter would be around 3 mm. EPMA analysis was performed every tenth of a mm. Consequently, graphs are presented so that each point is the average composition of the 10 closest points. One can notice the central part located at the crossing of the lines 1 and 3 is the most chemically homogenized zone. The corresponding microstructure is an intermediate microstructure between the one of zone B and the one of zone C (cf. Fig.1.a and c) and is fine enough. The composition in this zone can be calculated from the EPMA results and is around $\text{Al}_{73.2}\text{Cr}_{10}\text{Fe}_{5.3}\text{Mo}_{11.6}$. Matter to evaporate was then taken from this zone which is schematized in Fig. 1.a (grey central part).

3.2 Chemical and structural analysis of the films

A serie of films was prepared setting the distance d and substrate temperature T_s at different values: $d = 6, 9$ and 13 cm, $T_s = 285$ and 325 °C (Table 1 compiles all the experiments).

All films are nano-crystallized as the TEM dark field micrograph taken from the film prepared at $T_s = 325$ and $d = 9$ cm stands for (Fig. 2). Size of crystallites ranges from 2 to 70 nm. Average size of particles inside films increase with increasing T_s and d .

Two types of TEM diffraction patterns were obtained: one type (type I) exhibits rings that could be identified as the one of the O_1 phase as Fig. 3(a) shows. The O_1 phase is an orthorhombic phase, of Bmm2 space group. It was first discovered in the Al-Cr-Cu-Fe diagram by Dong and Dubois [22] and identified as an approximant of a Al-Cr-Cu-Fe quasicrystalline decagonal phase [22, 23]. The O_1 phase was also noticed in the Al-Cr-Fe diagram [15, 21]. The second type of TEM diffraction patterns (type II) exhibits fcc-Al dotted rings with traces of O_1 -ring like pattern of Fig. 3(b) shows it. Table 1 gives the type of pattern we have obtained versus the two process parameters d and T_s . The Al rings of the type II film prepared at $d = 9$ cm and $T_s = 325$ °C are less continuous than the other ones and are punctuated by spots. This is the result of the bigger size of the Al crystallites when d

increases. Basically, according to TEM diffraction, all films are of type II except two films: the one prepared at low d (6 cm), low T_s (285 °C), and the one prepared at high d (13 cm), high T_s (325 °C).

GXRD results also show the patterns are of two types. First type of pattern exhibits only the peaks of the O_1 structure (type I, fig.4.a) and happens only when $d = 6$ cm and $T = 285^\circ\text{C}$. The parameters found here for the O_1 structure are $a = 2.46 \pm 0.04$ nm, $b = 1.28 \pm 0.04$ nm and $c = 3.37 \pm 0.04$ nm, to be compared with $a = 3.25$ nm, $b = 1.25$ nm and $c = 2.36$ nm for O_1 -Al-Cr-Cu-Fe [22, 23] and with $a = 2.37$ nm, $b = 1.23$ nm and $c = 3.25$ nm for the O_1 -Al-Cr-Fe [15, 21]. Second type of pattern informs that the films prepared in the other conditions and even the one prepared at $d = 13$ cm, $T_s = 325$ °C, contain two phases: the O_1 phase and the face centred cubic Al phase (Fig.4.b) For clear understanding of the GXRD patterns: signal produced by the glass substrate itself before any deposition has been recorded and can be seen on Fig. 4(c). Analysed volume by GXRD is bigger than by TEM diffraction. This means that the TEM diffraction analysis has missed the Al grains because of their dispersion, and that at high substrate temperatures, big distances between the source and the substrate lead to films whose homogeneity is apparently of poorer quality than for the other conditions.

One concludes that all the films are made of mixed phases (type II) cubic aluminium and O_1 approximant, except one film which is pure and made of the O_1 phase only (type I). The O_1 pure film can be obtained by setting a small distance between the source and the substrate and by setting the substrate temperature at 285 °C.

The influence of d and T_s can then be synthesized: the smallest d is, the most homogeneous are the films. This can be linked to the angular dispersion of matter from the source during the evaporation. High substrate temperatures lead to films composed of approximant phase mixed with metallic f.c.c. aluminium. Above all, the way to get a pure approximant film is to take a small distance and a small temperature.

The chemical composition and in-depth chemical profiles were checked by SNMS analyses. All the profiles (either type I or II) look alike as the SNMS profile of the type I film ($d = 6\text{ cm}$, $T_s = 285\text{ }^\circ\text{C}$) stands for (Fig. 5). Transverse compositions of elements are not constant all along the depth. Net and progressive increase (respectively decrease) of Al (Cr, Fe and Mo) with increasing depth can be observed. All the films also exhibit a superficial zone of about 5 to 10 nm in thickness where oxidation and species diffusion seem to have occurred. Composition of the films was then calculated on the whole thickness without taking in account the superficial layer affected with oxidation and diffusion, giving average values. The type I film (pure O_1) is of $\text{Al}_{79}\text{Cr}_{12}\text{Fe}_7\text{Mo}_3$ composition. Compositions of the mixed films which do not correspond to any single phase, have then not been worked out. Taking the limits among the data presented in Fig. 5, one may conclude that the solid solution O_1 presents an existence domain ranging at least from 65 to 87% for Al, 9 to 14 % for Cr, 4 to 12 % for Fe and 0 to 8 % for Mo. Experimental error on composition analysis being 5%, one concludes that the solubility of Mo in the O_1 phase is at least of about few atomic %.

3.3 Optical reflectance

The optical reflectivity curves of the as-deposited pure O_1 film and the one of the polished $\text{Al}_{74}\text{Cr}_{10}\text{Fe}_6\text{Mo}_{10}$ ingot, used for making the films, are presented in figure 6. As expected of approximant materials [11, 14-15], one can see the obtained approximant film and the ingot effectively reflect around 60% of light over the infra-red domain. This result is similar to the one recorded on massive Al-Cr-Fe approximant samples made of a mixture of approximant phases by Demange et al. [14] and informs that the insertion of Mo inside the O_1 phase does not alter its optical behaviour.

The work should have to be completed by a study on the influence of the Mo on the corrosion resistance. Indeed, Al-Cr-Fe samples have been proved to behave excellently [15,16] and Mo influence in these specific films was not yet characterized.

5. Conclusion

The following important issues were pointed out in our study:

- Al-Cr-Fe-Mo films have been prepared and systematically analyzed. They are all continuous and small-grained (nanometer size). Films are generally homogeneous except at high d , high T_s .
- Most films are made of O_1 -phase and fcc-Al phase (approximant previously existing in Al-Cr-Fe and Al-Cr-Cu-Fe systems), one is purely composed of the O_1 -phase.
- Decorrelated and crossed influence of the temperature of the substrate and the distance between the source and the substrate have been worked out. Conditions of preparation for a film purely made of the O_1 -phase correspond to the smallest temperature and to the smallest distance tested.
- This work shows the O_1 -phase has an existence domain in the Al-Cr-Fe-Mo system.
- It also allowed us to determine the average lattice parameters of the O_1 -Al-Cr-Fe-Mo phase.
- Optical properties are conserved over the infra-red domain by the insertion of Mo in the Al-Cr-Fe system.

Acknowledgements

The authors would like to thank V. Demange for fruitful discussions, and J.-P. Houin for his excellent technical contribution on the temperature substrate device. The financial support

offered by Ministère de la Recherche et des Nouvelles Technologies under contract ERT
Quasicristaux Industriels is gratefully acknowledged.

References

- [1] J.- M. Dubois, S.S. Kang, Y. Massiani, *J. of non Cryst. Sol.*, 153-154 (1993) 443.

- [2] J.-M. Dubois, P. Weinland, French patent 2635117, 23/04/1993.

- [3] J.-M. Dubois, P. Archambault, B. Colleret, French patent 2685349, 25/03/1994.

- [4] T. Klein, O. G. Symbko, *Appl. Phys. Lett.* 64 (1994) 431.

- [5] N. Ichikawa, O. Matsumoto, T. Hara, T. Kitahara, T. Yamauchi, T. Matsuda, T. Takeuchi, U. Mizutani, *Jpn. J. Appl. Phys.* 33 (1994) 736.

- [6] A. Yoshida, K. Kimura, S. Takeuchi, *Jpn J. Appl. Phys.* 34 (1995) 1606.

- [7] C. Bergman, E. Emeric, P. Donnadiou, J. M. Dubois, P. Gas, in: C. Janot, R. Mosseri (Eds.), *World Scientific, Singapore (1996), Proceedings of the fifth International Conference on Quasicrystals, ICQ5, Avignon, France, May 22-26, 1995, p 774.*

- [9] C. Janot, J.-M. Dubois, “*Matières à Paradoxes*”, EDP Sciences, Les Ulis (France) 1998.

- [10] V. Brien, A. Dauscher, P. Weisbecker, F. Machizaud, *J. Appl. Phys. A* 76 (2003) 187.

- [11] J. Kong, C. Zhou, S. Gong, H.Xu, *Surf. and Coat. Technology*, 165 (2003) 281.

- [12] R. Teghil, L. D'Alessio, M. A. Simone, M. Zaccagnino, D. Ferro, D. J. Sordelet, J. Appl. Surf. Sci., 168 (2000) 267.
- [13] V. Demange, J.W. Anderegg, J. Ghanbaja, F. Machizaud, D.J. Sordelet, M. Besser, P.A. Thiel, J.-M Dubois, Appl. Surf. Sci., 173 (3-4) (2001) 327.
- [14] V. Demange, A. Milandri, M.-C de Weerd, F. Machizaud, G. Jeandel, J.-M. Dubois, Phys. Rev. B. (14) (2002) 6514.
- [15] V. Demange, F. Machizaud, J.-M Dubois, J.-W. Anderegg, P.-A. Thiel, D.-J. Sordelet, J. Alloys and Comp., 342, 1-2, (2002) 24.
- [16] L. Johann, A.E. Naciri, L. Broch, V. Demange, J. Ghanbaja, F. Machizaud, J.-M. Dubois, Appl. Surf. Sci., 207, 1-4, (2003) 300.
- [17] T. Eisenhammer, A. Mahr, A. Haugeneder, P. Reischelt, W. Assman, in: C. Janot, R. Mosseri (Eds.), World Scientific, singapore (1996), Proceedings of the fifth International Conference on Quasicrystals, ICQ5, Avignon, France, May 22-26, 1995, p 758.
- [18] T. Eisenhammer, H. Nelte, W. Assman, J.-M. Dubois, Mater. Res. Soc. Symp. Proc., vol 553, (1999) p 435.
- [19] T. Eisenhammer, M. Lazarov, German patent 4425140 (1994).
- [20] F. Machizaud, J.-M. Dubois, French patent 95.03939, 04/04/1995.

[21] V. Demange, J. S. Wu, V. Brien, F. Machizaud, J.-M. Dubois, Mater. Sci. Eng. 294-296, (2000) 79.

[22] C. Dong, J.-M. Dubois, J. Mater. Sci. , 26 (1991) 1647.

[23] C. Dong, J.-M. Dubois, S.S. Kang, M. Audier, Phil. Mag B., 65, 1, (1992) 107.

Figures captions

Figure 1: Characterization of the ingot containing the source matter to be evaporated. a/ Schematized cross section of the ingot. Localization of the lines analyzed by EPMA (Axis 1, 2 and 3), localization of the SEM micrographs (Zones A, B and C), grey part is the zone where matter was taken from, b/ EPMA chemical profiles (axis 1, 2 and 3) after 3 consecutive melting, each point is the average of the 10 closest points (precision of measurements is 1 at. %), c/ SEM micrographs showing the microstructure of the zones A, B and C (see a/). Precision of chemical composition is 1 at. %.

Figure 2: TEM Dark field image showing the nanosized granular morphology of a film elaborated at $d = 9$ cm, $T_s = 325$ °C (see table 1)

Figure 3: TEM Diffraction patterns. a/ Type (I) film made of O_1 phase only ($d = 6$ cm, $T_s = 285$ °C, see table 1), b/ Type (II) film made of pure Al and traces of O_1 phase ($d = 9$ cm, $T_s = 285$ °C, see table 1).

Figure 4: 0.5° incidence GXRD patterns, a/ film deposited at $d = 6$ cm, $T_s = 285$ °C, b/ film deposited at $d = 13$ cm, $T_s = 325$ °C (see table 1), c/ glass substrate prior to any deposition. Strikes indicate the positions of the O_1 2θ Bragg peaks.

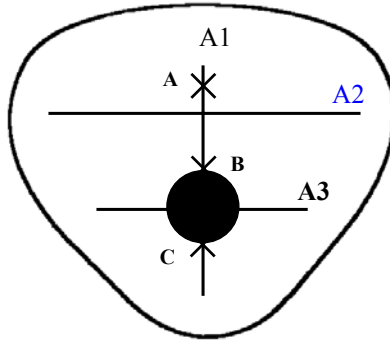
Figure 5: SNMS graph showing the composition of the pure approximant O_1 film across its depth ($d = 9$ cm, $T_s = 285$ °C, see table 1). Precision of measurements is 5 at. %.

Figure 6: Room temperature reflectance curves over the visible and infra-red domain of the pure approximant O_1 film and of the ingot taken for evaporation.

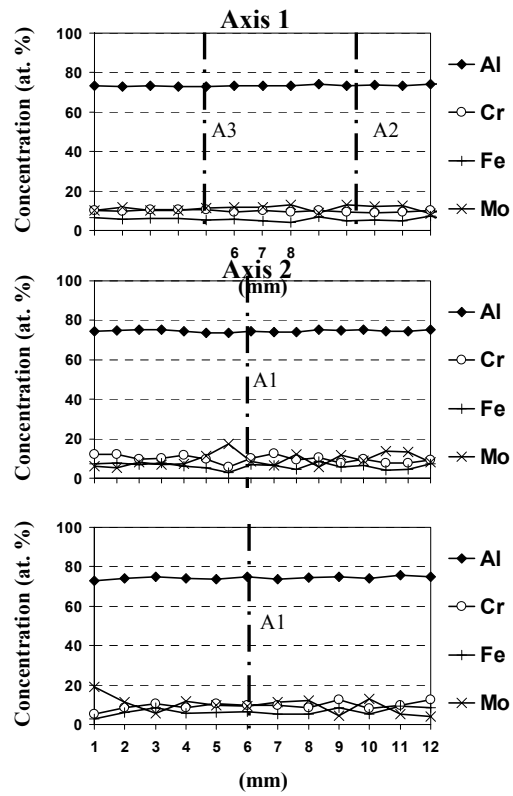
Table captions

Table 1

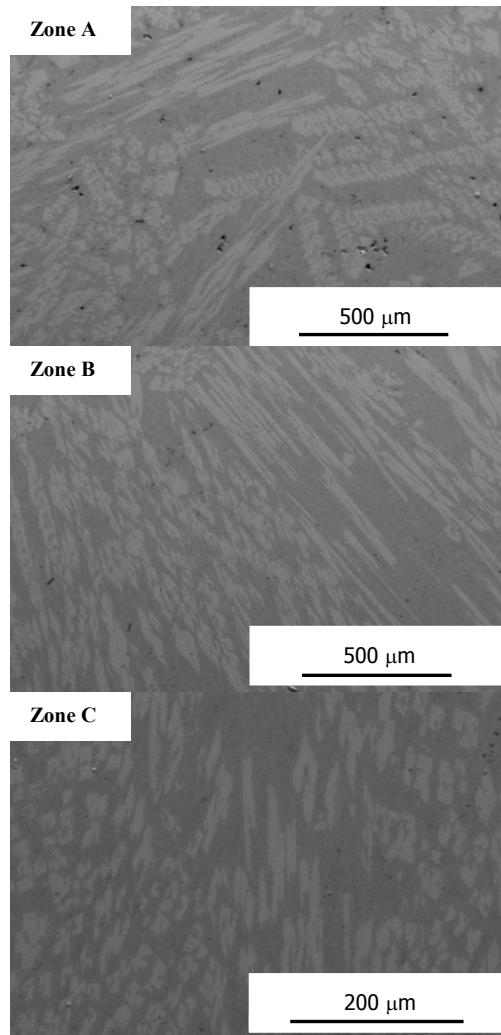
Identification of the phases present inside all the films prepared for this study according to the two diffraction techniques: grazing X-ray and electron diffraction. Type I = O_1 phase, type II = face centred cubic aluminium + O_1 phase, T_s : temperature of the substrate, d : distance between the source and the substrate.



a/

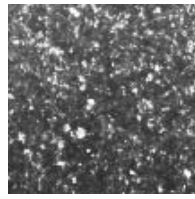


b/



c/

Figure 1



300 nm

Figure 2

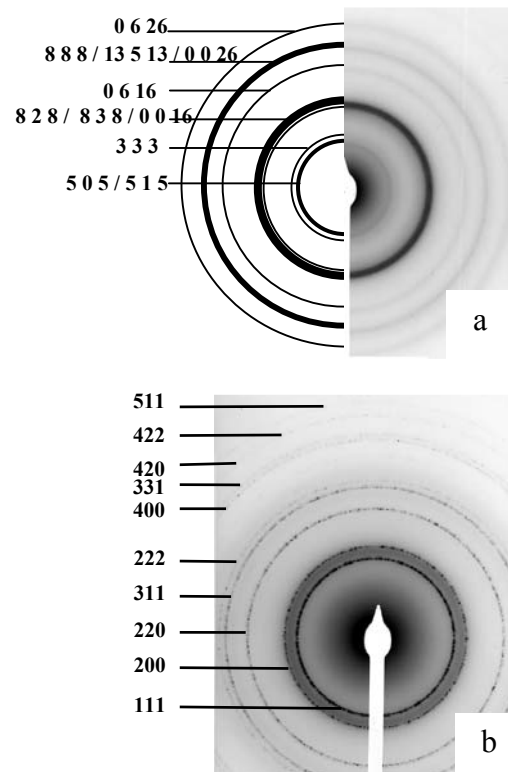


Figure 3

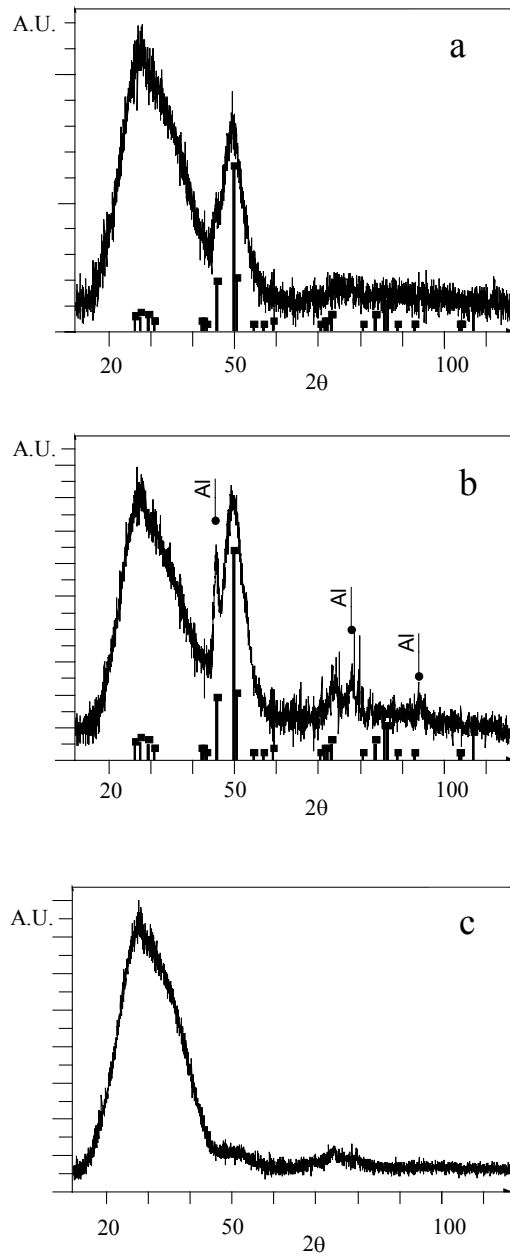


Figure 4

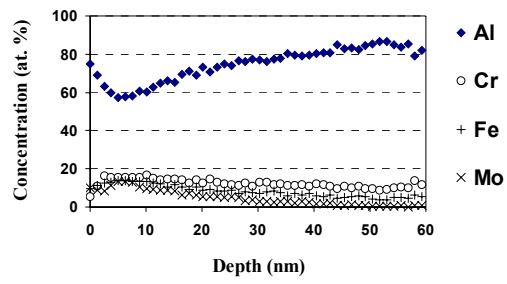


Figure 5

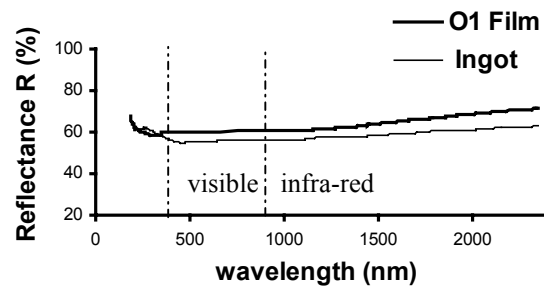


Figure 6

Tables

Analysis technique	T _s (°C)	d = 6 cm	d = 9 cm	d = 13 cm
TEM	325	II	II	I
	285	I	II	II
GXR	325	II	II	II
	285	I	II	II

Table1